Influence of Initial Order on the Microscopic Mechanism of Electric Field Induced Alignment of Block Copolymer Microdomains

Kristin Schmidt,[†] Alexander Böker,[*,†,‡] Heiko Zettl,[†] Frank Schubert,[†] Helmut Hänsel,[†] Franz Fischer,[§] Thomas M. Weiss,[⊥] Volker Abetz,[∥] A. V. Zvelindovsky,[*,#,¶] G. J. A. Sevink,[⊕] and Georg Krausch[*,†,○]

Lehrstuhl für Physikalische Chemie II, Universität Bayreuth, D-95440 Bayreuth, Germany, Lehrstuhl für Kristallographie, Universität Bayreuth, D-95440 Bayreuth, Germany, European Synchrotron Radiation Facility (ESRF), F-38043 Grenoble, France, GKSS−Forschungszentrum Geesthacht GmbH, Institut für Polymerforschung, Max-Planck-Strasse, D-21502 Geesthacht, Germany, Centre for Materials Science, Department of Physics, Astronomy & Mathematics, University of Central Lancashire, Preston PR1 2HE, United Kingdom, and Leiden Institute of Chemistry, Universiteit Leiden, P.O. Box 9502, 2300 RA Leiden, The Netherlands

Received May 20, 2005. In Final Form: July 7, 2005

We investigate the mechanism of microdomain orientation in concentrated block copolymer solutions exposed to a dc electric field by in situ synchrotron small-angle X-ray scattering (SAXS). As a model system, we use concentrated solutions of a lamellar polystyrene-*b*-polyisoprene block copolymer in toluene. We find that both the microscopic mechanism of reorientation and the kinetics of the process strongly depend on the initial degree of order in the system. In a highly ordered lamellar system with the lamellae being aligned perpendicular to the electric field vector, only *nucleation and growth of domains* is possible as a pathway to reorientation and the process proceeds rather slowly. In less ordered samples, *grain rotation* becomes possible as an alternative pathway, and the process proceeds considerably faster. The interpretation of our finding is strongly corroborated by dynamic self-consistent field simulations.

Introduction

Supramolecular self-assembly has recently become an area of increasing interest particularly due to its potential for large scale creation of nanostructured materials. Block copolymers are a prominent class of such materials as they spontaneously form ordered mesostructures of different symmetry (lamellae, hexagonally packed cylinders, and cubic lattices of spheres) with characteristic length scales in the 10−100 nm regime. In view of potential applications, however, the control of long-range orientational order and the removal of defects remains a crucial issue. Here, the manipulation or guidance of the spontaneous processes by application of controlled external fields (e.g., mechanic, electric, magnetic) proves to be a promising approach. Rather straightforward, *macroscopic* experiments (shear cells, capacitors, magnets) have proven successful to create long range order in the block copolymer *nano*structures.[1−5]

Owing to the different dielectric properties of the two blocks, an orientation of block copolymer microdomains parallel to an external electric field is energetically favored. The orientation of block copolymer microdomains by means of an electric field has been shown to be feasible with field strengths ranging from one to several tens of volts per micrometer, depending on the difference between the dielectric constants. Recent experiments and computer simulations have shown that two distinctly different microscopic pathways are possible when an ordered block copolymer mesostructure of arbitrary orientation is exposed to an external electric field.[6−8] In the case of sufficiently weak segregation between the two blocks, local nuclei of the favored parallel orientation are created. Subsequently, these nuclei grow. Consequently, in a scattering experiment, only the initial and the final orientations are observed with the intensity of the latter growing on expense of the former. Alternatively, in the case of stronger segregation between the respective blocks, the orientation of entire grains rotates, mediated by movement of individual defects perpendicular to the microdomain structure, until the favored orientation parallel to the field is reached. In this case, a scattering experiment will detect a continuous shift of the scattering pattern from the initial to the final orientation as has

* Corresponding authors.
† Lehrstuhl für Physikalische Chemie II, Universität Bayreuth.
‡ E-mail: alexander.boeker@uni-bayreuth.de.
§ Lehrstuhl für Kristallographie, Universität Bayreuth.
⊥ European Synchrotron Radiation Facility (ESRF).
∥ GKSS−Forschungszentrum GmbH.
University of Central Lancashire.
⊕ Universiteit Leiden.
○ E-mail: georg.krausch@uni-bayreuth.de.
¶ E-mail: avzvelindovsky@uclan.ac.uk.

(1) Thurn-Albrecht, T.; DeRouchey, J.; Russell, T. P.; Jaeger, H. M. *Macromolecules* **2000**, *33*, 3250−3253.
(2) Amundson, K.; Helfand, E.; Davis, D. D.; Quan, X.; Patel, S. S.; Smith, S. D. *Macromolecules* **1991**, *24*, 6546−6548.
(3) Böker, A.; Knoll, A.; Elbs, H.; Abetz, V.; Müller, A. H. E.; Krausch, G. *Macromolecules* **2002**, *35*, 1319−1325.
(4) Ebert, F.; Thurn-Albrecht, T. *Macromolecules* **2003**, *36*, 8685−8694.
(5) Keller, A.; Pedemonte, E.; Willmouth, F. M. *Nature (London)* **1970**, *225*, 538−539.
(6) Böker, A.; Elbs, H.; Hänsel, H.; Knoll, A.; Ludwigs, S.; Zettl, H.; Zvelindovsky, A. V.; Sevink, G. J. A.; Urban, V.; Abetz, V.; Müller, A. H. E.; Krausch, G. *Macromolecules* **2003**, *36*, 8078−8087.
(7) Böker, A.; Elbs, H.; Hänsel, H.; Knoll, A.; Ludwigs, S.; Zettl, H.; Urban, V.; Abetz, V.; Müller, A. H. E.; Krausch, G. *Phys. Rev. Lett.* **2002**, *89*, 135502.
(8) Zvelindovsky, A. V.; Sevink, G. J. A. *Phys. Rev. Lett.* **2003**, *90*, 049601.

10.1021/la051346w CCC: $30.25
Published on Web 08/23/2005

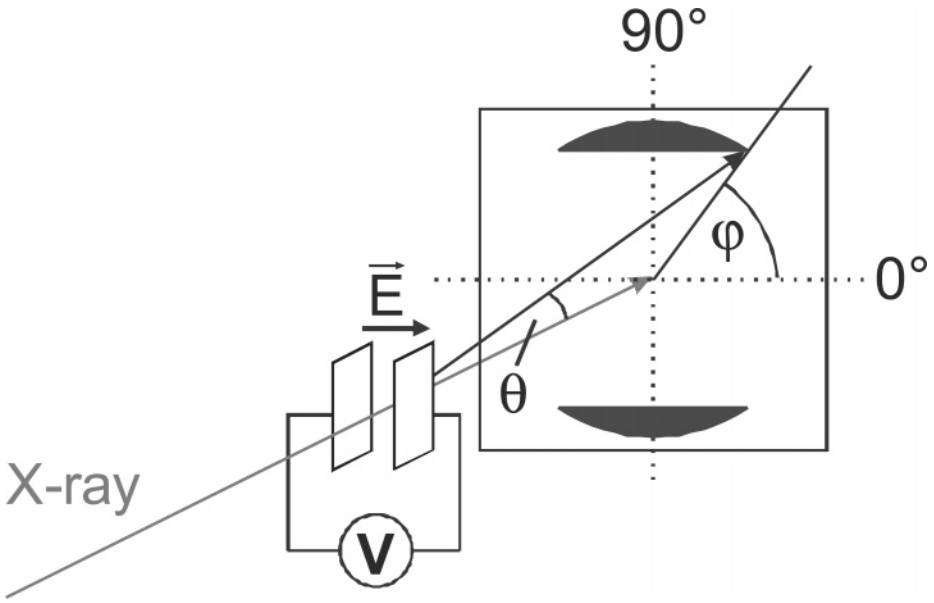

Figure 1. Experimental setup for *in situ* SAXS.

been found for electric field as well as for shear alignment.[7,9]

While the above considerations hold for bulk samples, in thin films additional effects come into play. Both lamellar and cylindrical mesophases in block copolymers preferentially align parallel to any boundary surface as such alignment typically decreases the interfacial energy of the structure with the boundary surface. In the case of a plate capacitor, these effects counteract the effect of the electric field which points perpendicular to the boundary surfaces. In consequence, a minimum electric field strength (*threshold* electric field strength) is required to overcome the parallel interfacial alignment.[10−13] Moreover, it has been shown that close to the electrodes the parallel alignment may prevail even if the bulk of the film is oriented perpendicular to the interfaces, resulting in a *mixed orientation of grains*. This even holds for shear aligned samples where the effective forces on the lamellae are much larger than in the electric field case.[14,15] While the thermodynamics of this competition is widely understood, the influence of the initial degree of order and initial orientation with respect to the boundary surfaces on the microscopic pathway leading to microdomain reorientation has barely been studied. This is even more surprising given the obvious importance of defect density and initial degree of order for the reorientation process as has been described for shear alignment experiments. Grain rotation relies on the movement of individual defects and therefore should strongly depend on the defect density. For the nucleation of grains of preferred orientation on the other hand, both structural defects as well as thermal fluctuations may serve as nuclei. Onuki and Fukuda have pointed out that undulation instabilities in lamellae in an oblique electric field will only develop if the angle between the plane of the lamellae and the electric field vector is sufficiently large.[16] Therefore, not only the defect density but also the degree of orientation and the angle between the microdomains and the electric field should be of importance.

In the present study, we have investigated in detail the influence of the degree of initial order on the microscopic route toward domain alignment. In a plate capacitor arrangement, we vary the plate spacing between 3.8 and 0.3 mm. The microdomains align parallel to the capacitor plates and the degree of order improves with decreasing capacitor spacing. At the same time, the process of reorientation slows down by about an order of magnitude as the capacitor spacing is reduced. Moreover, above a certain degree of order, described by the orientational order parameter P_2, grain rotation is completely suppressed and domain reorientation can only be achieved via nucleation and growth. Dynamic self-consistent field simulations corroborate that the different behavior is due to differences in the initial degree of order, which in turn increases with decreasing spacing between the capacitor plates.

Experimental Section

Synthesis. A polystyrene-*b*-polyisoprene block copolymer with a total number-average molecular weight $M_n = 100$ kg/mol was synthesized by sequential living anionic polymerization as described in detail elsewhere.[17] The polymer used in this study consists of 50 wt % polystyrene and 50 wt % polyisoprene (93% 1,4-cis microstructure, denoted as $S_{50}I_{50}^{100}$). Gel permeation chromatography (GPC) of the final block copolymer yields a polydispersity $M_w/M_n = 1.02$. The block ratio and overall molecular weight were determined by ^{1}H NMR using the integrated aromatic signals of the polystyrene block in combination with the GPC results of the corresponding polystyrene precursor.

Sample Preparation. Block copolymer solutions of 35, 50, and 55 wt % in toluene were prepared. The alignment experiments were performed in a home-built capacitor with gold electrodes (sample depth = 5 mm, electrode distance $d = 0.3$−3.8 mm) at room temperature. A dc voltage between 0.3 and 3.8 kV was applied across the capacitor resulting in a homogeneous electric field pointing perpendicular to the X-ray beam direction (Figure 1). Both the voltage at the electrodes and the current through

(9) Polis, D. L.; Smith, S. D.; Terrill, N. J.; Ryan, A. J.; Morse, D. C.; Winey, K. I. *Macromolecules* **1999**, *32*, 4668−4676.
(10) Xu, T.; Hawker, C. J.; Russell, T. P. *Macromolecules* **2003**, *36*, 6178−6182.
(11) Xu, T.; Zhu, Y.; Gido, S. P.; Russell, T. P. *Macromolecules* **2004**, *37*, 2625−2629.
(12) Tsori, Y.; Andelman, D. *Macromolecules* **2002**, *35*, 5161−5170.
(13) Lyakhova, K. S.; Zvelindovsky, A. V.; Sevink, G. J. A. In *AIP Conference Proceedings*; Tokuyama, M., Oppenheim, I., Eds.; 2004; Vol. 708, pp 217−220.
(14) Laurer, J. H.; Pinheiro, B. S.; Polis, D. L.; Winey, K. I. *Macromolecules* **1999**, *32*, 4999−5003.
(15) Winey, K. I.; Patel, S. S.; Larson, R. G.; Watanabe, H. *Macromolecules* **1993**, *26*, 4373−4375.
(16) Onuki, A.; Fukuda, J. *Macromolecules* **1995**, *28*, 8788−8795.
(17) Schmalz, H.; Böker, A.; Lange, R.; Krausch, G.; Abetz, V. *Macromolecules* **2001**, *34*, 8720−8729.

the sample were monitored during the course of the experiment. Within the sensitivity of the setup ($I \approx 0.01$ mA), no leakage currents were detected after the electric field was applied.

Synchrotron Small-Angle X-ray Scattering (Synchrotron-SAXS). Synchrotron-SAXS measurements were performed at the ID02 beamline at the European Synchrotron Radiation Facility (ESRF, Grenoble, France). The operating beam energy was 12.5 keV, corresponding to a peak wavelength of 0.1 nm. The beam direction (cross section: 100×100 μm^2) was perpendicular to the direction of the applied electric field. The detector system is housed in a 10 m evacuated flight tube. An image intensified CCD detector was used, which can handle the full X-ray flux. The CCD is capable of acquiring up to 10 frames of 1024×1024 pixels per second and a sequence of up to 120 frames can be acquired with this time resolution. Prior to data analysis, background scattering was subtracted from the data and corrections were made for spatial distortions, the detector efficiency, and beamstop.

Deconvolution of Reorientation Processes/Kinetic Analysis. In earlier studies,[3,6,7] we have quantified the orientation processes by calculating the orientational order parameter and fitting the respective plot of P_2 vs time to give a characteristic time constant τ. One may argue that this procedure is not satisfactory as it neglects the fact that the reorientation process is based on two quite different microscopic pathways (*grain rotation* and *nucleation and growth*, see Supporting Information, Suppl.-Figure 1). To quantify the overall kinetics of the present experimental series in more detail, we therefore used two Voigt-based fitting models, separately describing the characteristics of *nucleation and growth* and *rotation of grains* to simultaneously fit the overall azimuthal scattering pattern. *Nucleation and growth* is characterized by the appearance of a new peak at the final position, which grows on expense of the initial peak as a function of time. *Grain rotation*, on the other hand, is characterized by a continuous shift of the peak position from the initial to the final orientation. The deconvoluted scattering patterns were evaluated either by using the orientational order parameter or both the peak area (nucleation and growth) and angular shift of the peak maxima (rotation of grains). Examples of such deconvolution processes are shown as Supporting Information. In general, we can draw the following conclusions:

I. At the early and late stages, the two processes cannot be distinguished quantitatively as the peak intensities decrease (early stage) or grow (late stage) while the position of the peaks shift; i.e., the rotating grains grow in size and number during the orientation process.

II. Comparison between the typical time constant of rotation and nucleation and growth for a certain overall process are identical within the error of the fitting procedure.

III. The orientation processes are interlinked with each other such that the kinetics of the governing mechanism tends to dictate the kinetics and thus the rate of the resulting overall reorientation process.

We therefore decided to fit the overall process with a single time constant and use the result as a relative measure to compare the kinetics of the observed processes in dependence on the initial orientation. We quantify the orientation using the previously established process by calculating the order parameter P_2 according to eqs 1 and 2 as follows:[6]

$$P_2 = \frac{3\langle \cos^2\varphi \rangle - 1}{2} \tag{1}$$

with

$$\langle \cos^2\varphi \rangle = \frac{\int_0^{2\pi} d\varphi (I_q(\varphi)\cdot \cos^2(\varphi)\cdot |\sin(\varphi)|)}{\int_0^{2\pi} d\varphi (I_q(\varphi)\cdot |\sin(\varphi)|)} \tag{2}$$

Depending on the type of alignment, two different ranges of the order parameter exist. For lamellar alignment parallel to the electrodes (maximum scattering intensity at $\varphi = 0°$), P_2 ranges from 0 to 1 with $P_2 = 1$ corresponding to perfect lamellar alignment parallel to the electrodes. For an alignment of the lamellae along the field direction (maximum scattering intensity at $\varphi = 90°$), P_2 ranges from 0 to -0.5 with $P_2 = -0.5$ corresponding to the fully oriented case. Full orientation, however, still allows for an isotropic distribution of the lamellae normals in the plane of the electrodes.

To quantify the orientation kinetics, the orientational order parameter P_2 was calculated for each single scattering pattern acquired during the course of the experiment. The behavior of P_2 as a function of time t could be fitted by a single exponential as described by

$$P_2(t) = P_{2,\infty} + (P_{2,0} - P_{2,\infty})\, e^{-t/\tau} \tag{3}$$

with $P_{2,0}$ and $P_{2,\infty}$ being the limiting values of the order parameter before application of the electric field and at late times, respectively, and τ being the time constant.

Computer Simulation. We employ the dynamic self-consistent field theory, which describes the dynamic behavior of each molecule (modeled as Gaussian chains) in the mean-field of all other molecules.[18,19] The phase separation can be monitored by the scalar $\psi(\mathbf{r},t)$, which is the deviation of the number density of monomers of one type from its average value. In the case of an incompressible diblock copolymer melt the system is described by only a single density. Simulating a diblock copolymer solution requires an extra density for the solvent; however, we use a simplified model in the present study. It was shown theoretically that a block copolymer melt can serve as a good approximation to describe general features of phase behavior of concentrated block copolymers solutions with nonselective good solvents.[20] As we have shown recently, such description is well justified and gives an excellent agreement with experiments in the case of a nonselective or almost nonselective solvent.[21] The time evolution of the system in the simplest case follows a diffusion equation:[22]

$$\dot{\psi} = M\nabla^2 \mu + \eta \tag{4}$$

with the constant mobility M, and the thermal noise η.[19] The chemical potential in the presence of an electric field $\mathbf{E}$ has the form $\mu = \mu^0 - (\partial\epsilon/\partial\psi)_T E^2/8\pi$,[23] where μ^0 is the chemical potential in the absence of the electric field, and ϵ is the dielectric constant of the polymeric material, which can be approximated as $\epsilon \approx \epsilon_0 + \epsilon_1\psi$. The electric field inside the material $\mathbf{E}$ deviates from the applied electric field $\mathbf{E}_0 = (0,0,E_0)$ and can be written via an auxiliary potential as $\mathbf{E} = \mathbf{E}_0 - \nabla\varphi$. The potential is related to ψ via the Maxwell equation div $\epsilon\mathbf{E} = 0$. Keeping only leading terms, one can rewrite eq 4 in the form[8]

$$\dot{\psi} = M\nabla^2\mu^0 + \alpha\nabla_z^2\psi + \eta, \quad \alpha \equiv ME_0^2\frac{\epsilon_1^2}{4\pi\epsilon_0} \tag{5}$$

The chemical potential without the electrostatic contribution μ^0 is calculated using self-consistent field theory for the ideal Gaussian chains with the mean field interactions between copolymer blocks A and B, described by a parameter ϵ_{AB}.[18]

The model system we study in the following is a symmetric A_4B_4-copolymer melt. The simulations have been performed in a two-dimensional box with 256×256 grid points and periodic boundary conditions.[18] For the simulations, the electric field strength is parametrized by $\tilde{\alpha} \equiv \alpha/kTM\nu$,[8,13] where ν is a polymer chain volume. The samples were shear-aligned with the dimensionless shear rate $\tilde{\dot{\gamma}} = 0.001$; for details please see ref 24.

(18) Sevink, G. J. A.; Zvelindovsky, A. V.; van Vlimmeren, B. A. C.; Maurits, N. M.; Fraaije, J. G. E. M. *J. Chem. Phys.* **1999**, *110*, 2250–2256.

(19) van Vlimmeren, B. A. C.; Maurits, N. M.; Zvelindovsky, A. V.; Sevink, G. J. A.; Fraaije, J. G. E. M. *Macromolecules* **1999**, *32*, 646–656.

(20) Fredrickson, G. H.; Leibler, L. *Macromolecules* **1989**, *22*, 1238–1250.

(21) Knoll, A.; Horvat, A.; Lyakhova, K. S.; Krausch, G.; Sevink, G. J. A.; Zvelindovsky, A. V.; Magerle, R. *Phys. Rev. Lett.* **2002**, *89*, 035501.

(22) Onuki, A. *Phase Transition Dynamics*; Cambridge University Press: Cambridge, U.K., 2002.

(23) Landau, L. D.; Lifshitz, E. M. *Electrodynamics of Continuous Media*; Pergamon: Oxford, U.K., 1960; Chapter II.

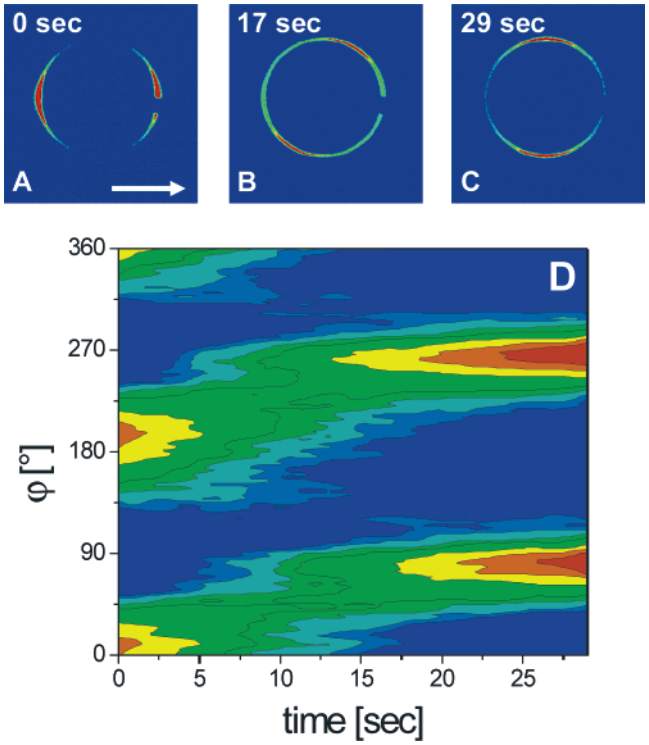

Figure 2. (A–C) Scattering images of a 35 wt % solution of $S_{50}I_{50}^{100}$ in toluene prior (A) and after (B, C) application of an electric field (1 kV/mm and $P_{2,0} = 0.46$). The arrow indicates the direction of the electric field vector. (D) 3D representation of the azimuthal angular dependence of the scattering intensity for the reorientation. The color code was chosen so that blue represents lowest intensity and red stands for the highest scattering intensity.

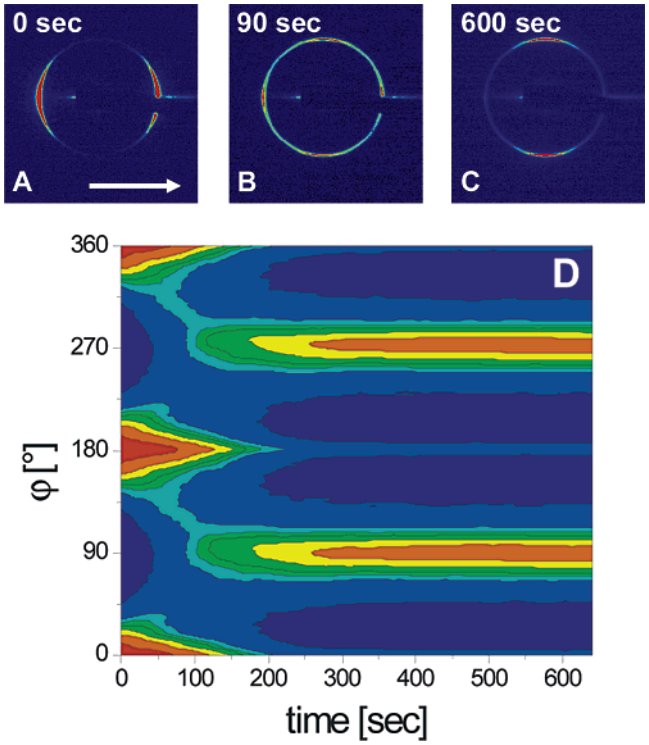

Figure 3. (A–C) Scattering images of a 35 wt % solution of $S_{50}I_{50}^{100}$ in toluene prior (A) and after (B,C) application of an electric field (1 kV/mm and $P_{2,0} = 0.83$). The arrow indicates the direction of the electric field vector. (D) 3D representation of the azimuthal angular dependence of the scattering intensity for the reorientation.

Results and Discussion

Using different capacitor spacings, we control the initial degree of order in the microdomain structures prior to application of the electric field. As we have noted earlier, the lamellae are exposed both to the shear fields occurring during sample preparation (the sample solution is filled into the capacitor via a syringe inserted at one side of the cell with an intake diameter corresponding to the electrode spacing) and to the surface fields favoring parallel alignment of the lamellae.[6] In consequence, the initial microdomain orientation is not random, but is preferentially aligned parallel to the capacitor plates. This alignment can easily be quantified through the orientational order parameter P_2 at $t = 0$.

We start our discussion with the kinetics of microdomain reorientation as followed in the center of the capacitor filled with a polymer solution with the lamellae oriented parallel to the electrodes exhibiting an initial degree of orientational order of $P_{2,0} = 0.46$. Figure 2 shows the 2D SAXS patterns in the absence of an external electric field (Figure 2A) and after exposure to the electric field for different times (Figure 2, parts B and C). Clearly, at short times an intermediate orientation is observed pointing to grain rotation as the dominant reorientation process. This is clearly visible in the time dependent plot of the azimuthal scattering intensity (Figure 2D) as well, which also shows that at least a major part of the scattering intensity is shifted continuously from the initial orientation at $\varphi = 0$ and 180°, respectively, to the final orientation at $\varphi = 90$ and 270°. This situation changes significantly

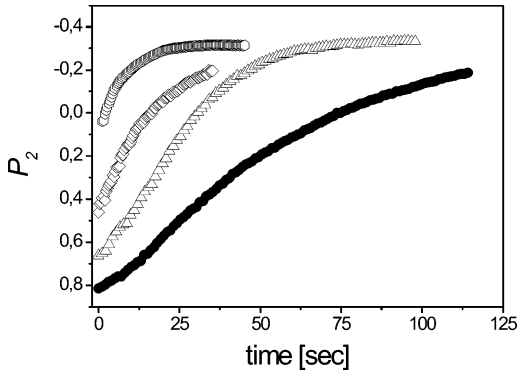

Figure 4. Kinetics of a 35 wt % solution of $S_{50}I_{50}^{100}$ in toluene at 1 kV/mm for different initial degrees of order. Evolution of the orientational order parameter: (⬡) $P_{2,0} = 0.04$ (R); (◇) $P_{2,0} = 0.46$ (R); (△) $P_{2,0} = 0.66$ (R); (●) $P_{2,0} = 0.83$ (NG) (NG = Nucleation and Growth; R = Rotation).

if we turn to samples with higher initial alignment. In Figure 3, we show the reorientation behavior of a polymer solution with $P_{2,0} = 0.83$. In contrast to the data shown in Figure 2, at any time only two distinct domain orientations are observed resulting in scattering peaks at $\varphi = 0$ and 180° (initial, Figure 3A) and at $\varphi = 90$ and 270° (final, Figure 3C). At intermediate times, both orientations coexist (Figure 3B), while almost no intermediate orientations are observed and only a negligible portion of the sample rotates. The time dependent plot of the azimuthal scattering intensity (Figure 3D) clearly shows the switching between the initial and the final orientation. This scattering behavior is indicative of nucleation and growth of grains of the final orientation. Grain rotation seems to be almost completely suppressed in this situation. It is interesting to quantify the kinetics of reorientation as a

(24) Zvelindovsky, A. V.; Sevink, G. J. A.; van Vlimmeren, B. A. C.; Maurits, N. M.; Fraaije, J. G. E. M. *Phys. Rev. E* **1998**, *57*, R4879–R4882.

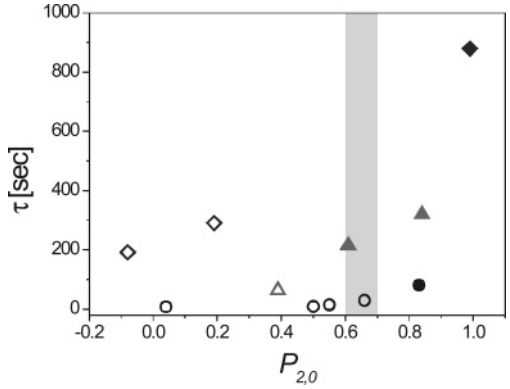

Figure 5. Experimental time constants τ as a function of the initial order parameter for solutions of $S_{50}I_{50}^{100}$ in toluene at 1 kV/mm: ◇ = 55 wt %, △ = 50 wt %, and ○ = 35 wt %. Full symbols relate to nucleation and growth as the dominant mechanism, while open symbols refer to grain rotation.

Table 1. Time Constants of the Reorientation Behavior at Different Values of $P_{2,0}$ Obtained from Fits Using Eq 3 (w_p = 35 wt %, E = 1 kV/mm) (NG = Nucleation and Growth; R = Rotation)

$P_{2,0}$	τ [s]	dominating mechanism
0.83	81.0	NG
0.66	29.6	R
0.55	15.0	R
0.50	9.0	R
0.04	7.8	R

function of $P_{2,0}$. In Figure 4 we show the time dependence of the P_2 values calculated from the raw data according to eq 1. Fitting a single exponential to the data (eq 3) yields time constants τ, which increase from τ = 7.8 s at $P_{2,0}$ = 0.04 to as much as τ = 81 s for $P_{2,0}$ = 0.83 (Table 1).

In Figure 5, we plot the kinetic data (τ values) as a function of the initial degree of order $P_{2,0}$ of the microdomains for 3 different block copolymer solutions (see Figure caption for details). Full symbols relate to nucleation and growth as the dominant mechanism, while open symbols refer to grain rotation. Only at sufficiently low degrees of order grain rotation is observed. We identify a minimum degree of initial order characterized by a $P_{2,0}$ value between 0.6 and 0.7, at which we observe a switch from rotation of grains to nucleation and growth. It therefore seems reasonable to assume that the degree of alignment (and, in turn, the defect density) has significant influence on the microscopic pathway for microdomain reorientation in the presence of the electric field.

The above interpretation is strongly corroborated by analysis of the real space data provided by computer simulations. We have performed two-dimensional dynamic self-consistent field simulations on lamellar diblock copolymer melts starting from two different initial conditions. In all cases the microdomain structure was first exposed to a shear field resulting in alignment of the lamellae in a well-defined direction to the electric field vector. Different shearing times and directions (A and B, perpendicular to the electric field vector; C, parallel to the electric field vector) were chosen in order to produce initial states of different degrees of alignment. The first copolymer system studied has mean field interactions ϵ_{AB} = 6 kJ/mol. It was found earlier to exhibit nucleation and growth as the dominant reorientation mechanism.[6,8] Initial microdomain structures created this way are shown in Figure 6 , parts A, B, and C. Indeed, as the electric field is applied, a distinctly different behavior is observed depending on the initial degree of alignment parallel to the electrodes. In the highly aligned sample with a largely dominant microdomain orientation perpendicular to the electric field vector (Figure 6A), the reorientation process is rather slow and proceeds exclusively via nucleation and

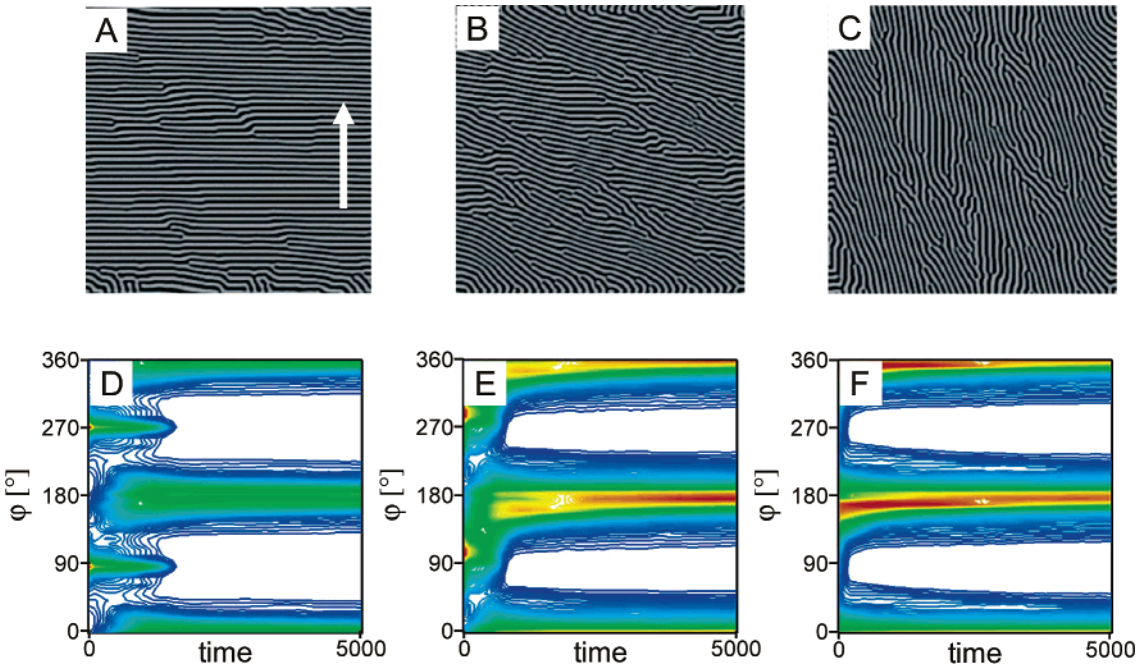

Figure 6. (A−C) Self-consistent field theory simulation of initial microdomain structure, prealigned using shear: (A) highly aligned sample (7500 time steps of shear perpendicular to electric field), (B) less aligned sample (2500 time steps of shear perpendicular to electric field), and (C) least aligned sample (2500 time steps of shear parallel to electric field). The arrow indicates the direction of the electric field vector. (D−F) Fourier transform squared of 2D simulated structures at dimensionless time t: (D) nucleation and growth mechanism for highly aligned sample, (E) combination of nucleation and growth mechanism and some grain rotation for the less aligned sample, and (F) solely grain rotation mechanism for the least aligned sample. The electric field strength is $\tilde{\alpha}$ = 0.2.

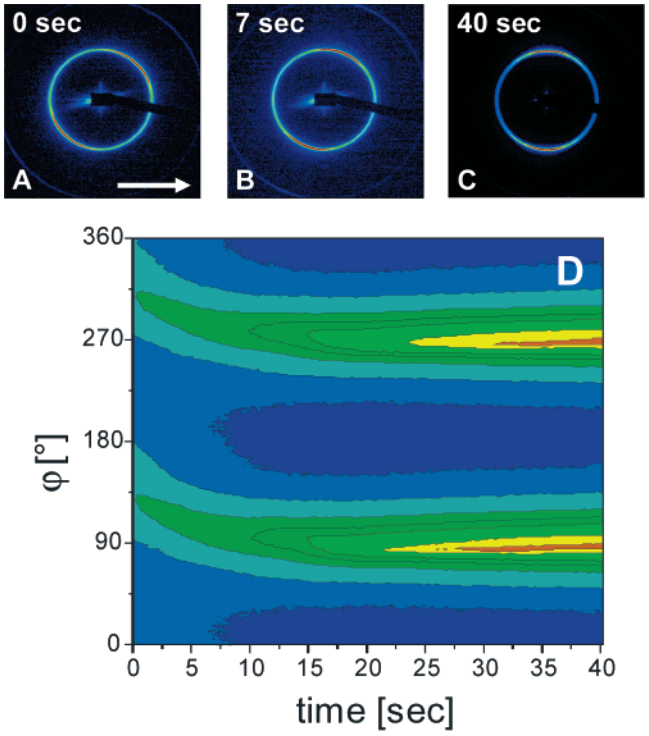

Figure 7. (A–C) Scattering images of a 35 wt % solution of $S_{50}I_{50}^{100}$ in toluene prior (A) and after (B, C) application of an electric field (1 kV/mm; $P_{2,0} = 0.04$). The arrow indicates the direction of the electric field vector. (D) 3D representation of the azimuthal angular dependence of the scattering intensity for the reorientation.

growth. The scattering functions calculated from these simulations are shown in Figure 6D and exhibit the same characteristic features seen in the experimental scattering intensity in Figure 3. In the less aligned sample (Figure 6B) reorientation is found to proceed faster and grain rotation increasingly contributes to the reorientation. This is seen in the scattering functions shown in Figure 6E, which resemble the experimental data found at large capacitor spacing (Figure 2). In the case of a structure even less aligned parallel to the electrodes, Figure 6C, the same copolymer system exhibits only grain rotation via movement of individual defects perpendicular to the lamellae. The scattering function in Figure 6F exclusively shows a shift of the peak, with no signs of nucleation and growth mechanisms present. This is very similar to what was observed for $P_{2,0} = 0.04$ as depicted in Figure 7, showing that the lamellae are less ordered and tilted toward the electric field lines. Obviously, consistent with the theory of Onuki et al.,[16] the initial angle between the lamella plane and the electric field vector is not sufficient for the instabilities in the structure to grow. Such instabilities are needed to nucleate grains of an orientation parallel to the external field. In this case, the only possible route to follow for the system is the rotation of grains, as it proceeds via individual defect movement. Moreover, at these intermediate orientations, the electric field induced torque acting on the lamellae increases with increasing lamellar misalignment with respect to the electrodes and reaches its maximum at a tilt angle of 45°.[23] Figure 8 provides a detailed real space view of the above-described processes. It can be seen in Figure 8A that even in the absence of defects in the initial structure in Figure 6A, grains of the new phase nucleate due to the growth of instabilities. The number of nuclei depends on the initial defect density (see Figure 8, parts A and B). The speed of the reorientation processes can be monitored by P_2 plots as shown in Figure 9, which qualitatively follow similar

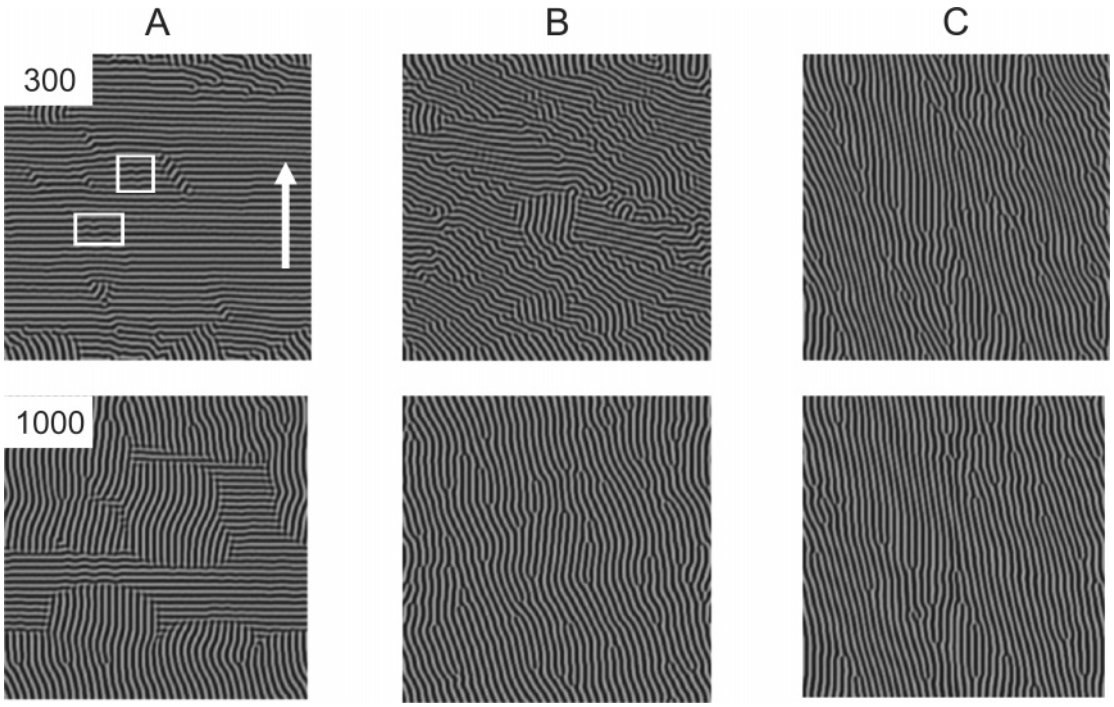

Figure 8. Self-consistent field theory simulation. Real space representation of reorientation mechanisms for different preoriented samples in Figure 6: (A) nucleation and growth mechanism for highly aligned sample (white frames highlight undulation instabilities and nucleation sites), (B) combination of nucleation and growth mechanism and some grain rotation for less aligned sample (lower left corner: rotation; center: nucleation and growth), and (C) solely grain rotation mechanism for the least aligned sample. Top row of snapshots is taken at the initial stages at dimensionless time $t = 300$ bottom row at time $t = 1000$. The arrow indicates the direction of the electric field vector.

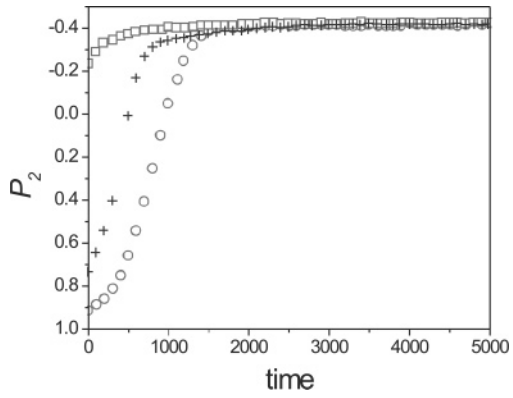

Figure 9. Order parameter for the systems in Figures 6 and 8 as a function of dimensionless time. P_2 is calculated from the 2D simulation images analogue eq 1 (with cos φ calculated directly from the density images using gradients in density) (A = ○, B = +, and C = □) as in Figures 6 and 8.

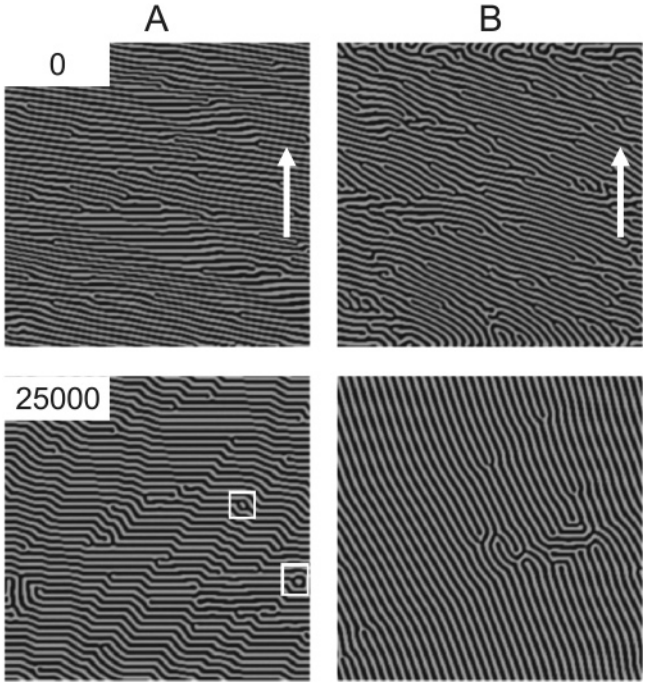

Figure 10. Self-consistent field simulation of a system exhibiting only grain rotation mechanism: (A) better aligned sample; (B) less aligned sample. Top row: initial structure. Bottom row: final structure at time $t = 25000$. The electric field strength is $\tilde{\alpha} = 0.2$. The arrow indicates the direction of the electric field vector. The white frames highlight typical defects for nucleation and growth.

trends as the experimental curves, as a function of initial alignment (see Figure 4).

In addition, we have also performed simulations for the copolymer system with mean field interactions $\epsilon_{AB} = 8$ kJ/mol, which was found earlier to reorient by the grain rotation mechanism only.[8] Figure 10A shows a total suppression of the rotation in the better aligned sample compared to the one in Figure 10B (the latter one is the same as in Zvelindovsky et al.[8]). The system in Figure 10A seemingly is trapped kinetically and only a few defects typical for nucleation and growth (white boxes) are generated slowly. This finding is consistent with the interpretation of the experiments mentioned earlier, that the rotation will be increasingly suppressed in a thinner slit, where lamellae are initially oriented more parallel to the electrodes.

Judging from the simulation results, we may indeed assume that the different degrees of initial order are responsible for the observed differences both in the kinetics and in the mechanism of reorientation. As can be seen from Figure 5, the process of reorientation becomes slower with increasing alignment and decreasing defect density. This is accompanied by a switch in mechanism from rotation of domains to nucleation and growth. Once the degree of initial order reaches a value of $P_2(t = 0) > 0.6$, grain rotation seems to be largely suppressed. For $P_2(t = 0) > 0.7$ grain rotation is no longer observed. Obviously, the number of defects in the microstructure becomes insufficient to support grain rotation by defect movement. Here, structural defects exclusively serve as nucleation centers for new domains. At the highest degrees of initial order, one is led to the assumption that the number of structural defects is too small to initiate sufficient nucleation centers. Therefore, thermal fluctuations of the lamellae amplified by the external electric field are needed for nuclei to be formed.

Conclusion

It has been found that both the reorientation pathway and the reorientation kinetics for lamellar microdomains in an external electric field strongly depend on the degree of order present prior to the application of the field. Samples of the same concentration but different initial order not only exhibit different mechanisms of orientation but also proceed at different rates. For intermediate degrees of order, where orientation proceeds via both pathways, we find that the dominating mechanism dictates the overall rate of reorientation. We observe consistently that for all systems rotation of lamellae by defect movement is faster than reorientation by nucleation and growth of new domains. On the basis of our results, we may conclude that above a certain initial orientation parallel to the electrodes the defect density and electric field induced torque are too low to allow for rotation of domains. In addition, the pressure on the well-aligned lamellae (as already pointed out by Onuki and Fukuda)[16] is larger than for less aligned samples and therefore leads to undulation instabilities which finally serve as nucleation centers for the growth of grains oriented parallel to the external electric field. This leads to a switch in orientation mechanism with increasing initial microdomain orientation from rotation to nucleation and growth.

Acknowledgment. The authors thank H. Krejtschi and his team for the skillful assistance in constructing the experimental setup and Oscar Lafuente and Gabi Cantea for assistance during the Synchrotron measurements. We are grateful to the ESRF for financial support and provision of synchrotron beam time. This work was carried out in the framework of the Sonderforschungsbereich 481 (TP A2) funded by the Deutsche Forschungsgemeinschaft (DFG) as well as of the Nederlandse Organisatie voor Wetenschapelijk Onderzoek (NWO)-DFG bilateral program. Supercomputer time was provided by Stichting Nationale Computerfaciliteiten (NCF).

Supporting Information Available: Figures showing the mechanism of the microdomain reorientation, deconvolution of the scattering intensity, a 3D representation of the angular dependence of the scattering intensity, the evolution of the order parameter P_2 with time, and text discussing the fitting model. This material is available free of charge via the Internet at http://pubs.acs.org.

LA051346W